Supporting Information

Hsp70 inhibits the nucleation and elongation of tau and sequesters tau aggregates with high affinity

Franziska Kundel[1], Suman De[1,2], Patrick Flagmeier[1,2], Mathew H. Horrocks[1], Magnus Kjaergaard[1,†], Sarah L. Shammas[1,†], Sophie E. Jackson[1], Christopher M. Dobson[1] and David Klenerman[1,*]

[1] Department of Chemistry, University of Cambridge, Lensfield Road, Cambridge CB2 1EW, United Kingdom.

[2] These authors contributed equally.

[†] Present addresses: Aarhus Institute of Advanced Studies, Høegh-Guldbergs Gade 6B, building 1630, 310, 8000 Aarhus C, Denmark; Department of Biochemistry, University of Oxford, South Parks Road, Oxford OX1 3QU.

[*] Correspondence should be addressed to dk10012@cam.ac.uk.

Table of Contents

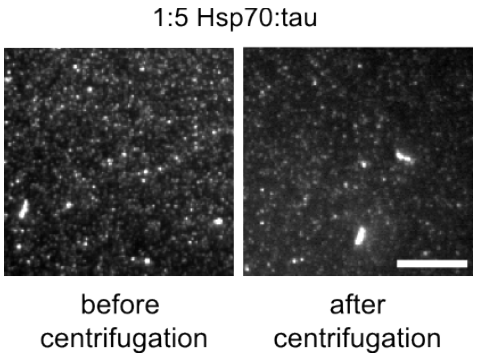

Supporting Figure 1: Small soluble tau aggregates formed in the presence of Hsp70

Tau was aggregated in the presence of Hsp70 (1:5 Hsp70:tau) for 24 hours and then the sample composition was analysed by TIRF microscopy using ThT to stain beta-sheet rich species. Small ThT-active aggregates detected by this method remain in the supernatant during centrifugation at 16,000 g (20 minutes).

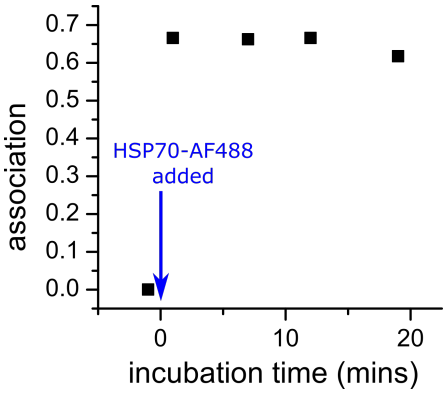

Supporting Figure 2: Fast on-rate of Hsp70 to tau aggregates

To ensure binding of Hsp70 to tau aggregates reached equilibrium conditions by the time of smFRET analysis, the on-rate of Hsp70 to tau was assessed. For this purpose, oligomeric tau was mixed with 1000 nM Hsp70-AF647 and the association was measured by smFRET after indicated periods of time. Complex association had reached maximum values within the experimental dead time (~1 minute), demonstrating fast binding kinetics of Hsp70 to tau oligomers. N=1.

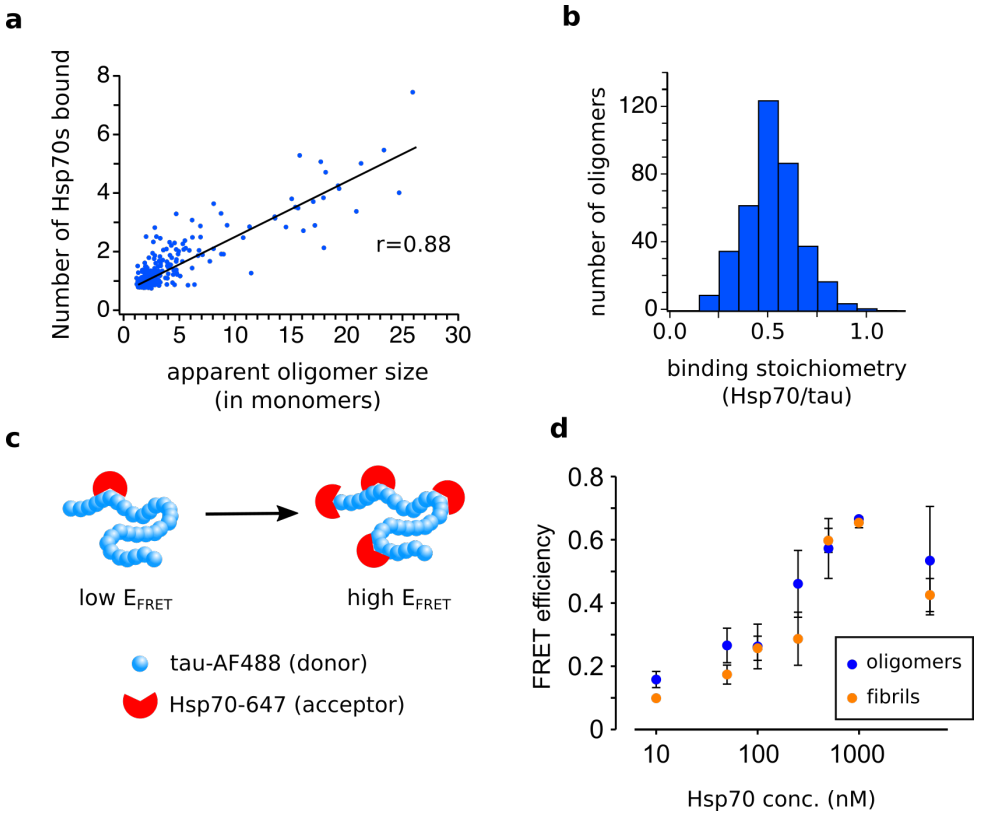

Supporting Figure 3: Stoichiometry of Hsp70 - K18 ΔK280 tau binding

a+b) Analysis of the binding stoichiometry of Hsp70-AF405 to tau oligomers from the TIRF microscopy images as shown in Fig. 4a. The number of Hsp70-AF405 molecules bound was calculated from the fluorescence intensity of a single Hsp70-AF405 molecule. a) The number of Hsp70 molecules correlates with the apparent oligomer size (Pearson's r=0.88). b) Representative histogram of binding ratio (Hsp70s per tau monomer incorporated into an oligomer).
c) Schematic of Hsp70-AF405 binding to tau aggregates. The FRET efficiency increases as the number of acceptors increase.
d) Average FRET efficiencies of tau-AF488/Hsp70-AF647 complexes as a function of Hsp70 concentration. N=3, error bars are s.e.m.

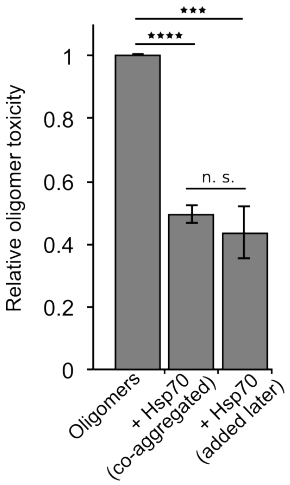

Supporting Figure 4: Tau oligomer toxicity after incubation with Hsp70

The relative toxicity of tau oligomers, untreated (column 1) or incubated with Hsp70 (columns 2 and 3), was tested using a single-vesicle permeabilization assay. Tau was either oligomerized in presence of Hsp70 (column 2), or Hsp70 was added to tau oligomers after the oligomerization process (column 3). Hsp70 neutralizes tau oligomer toxicity by about 50% in either case. Statistical test: One-way ANOVA; *** signifies $p \leq 0.001$, **** $p \leq 0.0001$.

Testing association and disassociation kinetics

In order to obtain binding saturation curves, first equilibrium or pseudo-equilibrium conditions must be achieved. To ensure the association of Hsp70 to tau aggregates had reached equilibrium conditions by the time of smFRET analysis, the association of Hsp70 to tau aggregates was first measured as a function of time. To perform this experiment, tau-AF488 was first oligomerized for 45 minutes. Note that the fraction of oligomers is around 10% in this sample as determined by smFRET. Then, this oligomeric tau sample was mixed with a high concentration of Hsp70-AF647 (1000 nM) and the association was measured by smFRET after indicated periods of time. Complex association had reached maximum values within the experimental dead time (~1 minute), demonstrating fast binding kinetics of Hsp70 to tau oligomers (see Figure S2). Next, the off-rate of Hsp70 from tau aggregates was assessed. As samples are highly diluted immediately prior to the smFRET analysis (5000-fold), complex dissociation can be a limiting factor for determining binding kinetics. However, association values close to 100% were obtained at high Hsp70 concentrations, indicating that the off-rate of the complex is orders of magnitude lower than the measurement time. Therefore, saturation binding curves were conducted under pseudo-equilibrium conditions.

Fitting kinetic data to obtain relative elongation rates

As described in detail previously[1,2], seeded experiments can be performed to sample the elongation process during aggregation separately from other processes. In the presence of preformed aggregates at high concentrations, the initial aggregation behavior is determined purely by the elongation of existing seeds. Specifically, the initial gradient is given by

$$\frac{dM}{dt} = 2k_+ m_0 P_0 \tag{1}$$

with M=aggregate mass concentration, k_+=elongation rate constant, P_0= aggregate number concentration and m_0=initial monomer concentration. At constant monomer concentration m_0 and constant aggregate number concentration P_0, the initial aggregation gradient can be used directly to extract the elongation rate constant k_+. In the seeded experiments performed here, P_0 is constant (as the same seed stock was used), but its values is not known, and therefore relative elongation rate constants k'_+ are shown to allow comparison between the different conditions (Hsp70 concentrations):

$$k'_{+,\mathrm{n}} = \frac{\left(\frac{dM}{dt}\right)_n}{\left(\frac{dM}{dt}\right)_1} = \frac{k_{+,n}}{k_{+,1}} \tag{2}$$

with n describing the different conditions (1=tau only, etc.). $(dM/dt)_n$ was obtained from linear regression of the initial aggregation kinetics (0.5-1.5h of aggregation).

Confocal smFRET data analysis

Studying the influence of Hsp70 on the oligomerisation of K18 ΔK280 tau by smFRET

Data analysis. The collected photon traces were analysed using a custom-written Igor Pro 6.22 (Wavemetrics) script as previously described[3]. To analyse the photon time traces the average auto-fluorescence for each channel (0.62 counts/bin for the donor channel and 0.59 counts/bin for the acceptor channel) was subtracted and the data was corrected for the spectral cross-talk from the donor channel into the acceptor channel (2 %). A threshold of 10 counts/bin for the donor and the acceptor channel was used to separate the photon burst-events from background as determined using dual-labelled DNA duplex. The number of donor events and oligomer events recorded per second (r_D and r_C, respectively) allows the calculation of the association quotient Q representing the fraction of dual-labelled molecules (aggregates)[4]:

$$\mathrm{Q} = \frac{1}{2}\frac{\mathrm{r_C}}{\mathrm{r_D}} \tag{3}$$

The ratio of the coincident event rate to the donor burst rate is divided by two to account for the acceptor bursts rate which cannot be measured directly. Therefore, it is assumed to be identical to the donor burst rate. Furthermore, the fraction of oligomers Q was further corrected for the efficiency of detection of coincidence fluorescence previously determined to be 25% using dual-labelled 40 bp-dsDNA[4]. Finally, the Q-value was corrected for the fact that oligomeric species containing either only donor or only acceptor molecules are not detectable by smFRET. Thus, a correction factor derived from the encounter probabilities according to Pascal's triangle was applied[5–7].

The FRET-efficiencies (proximity ratios) are calculated according to

$$E_{FRET} = \frac{I_A}{\gamma I_{DA} + I_A} \quad (4)$$

where I_A and I_{DA} correspond to the acceptor fluorescence intensity and to the donor fluorescence intensity in the presence of acceptor, respectively. γ is an instrument specific correction factor which accounts for different quantum yields and detection efficiencies of the donor and acceptor (0.65 here). FRET efficiencies were calculated for all events and combined in a FRET efficiency histogram[7].

The approximate number of monomers per oligomer event can be determined based on the average intensity from a blue monomer $I_{Dmonomer}$ according to the following equation

$$\text{apparent oligomer size} = 2\left(\frac{I_{DA} + \frac{I_A}{\gamma}}{I_{D_{monomer}}}\right) \quad (5)$$

Species occupying more than one bin e.g. due to increased size were excluded from analysis as they were assumed to be fibrillar events[7].

Measuring binding affinities of tau species to Hsp70

The collected photon traces were analysed as described above with the following adaptions. The association Q was calculated from the rate of donor events per second, r_d, and the rate of coincident FRET events per second, r_c:

$$Q = \frac{r_c}{r_d} \quad (6)$$

The Q-values obtained were then plotted as a function of total Hsp70 concentration to obtain saturation binding curves. To correct for ligand depletion and to account for the fact that the association was measured as a function of total Hsp70 concentration rather than the concentration of free Hsp70, fits were performed using the following equation[8]

$$Q = \frac{(A+B+K_d) - \sqrt{(A+B+K_d)^2 - 4AB}}{2} \quad (7)$$

where A is the total concentration of aggregates, B is the total concentration of Hsp70 and K_d is the dissociation constant.

The apparent aggregate size was determined from the average donor monomer intensity, $I_{D_{monomer}}$, and the sum of the acceptor fluorescence intensity, I_A, and to the donor fluorescence intensity in the presence of acceptor, I_{DA}, respectively:

$$\text{Apparent oligomer size} = \left(\frac{I_{DA} + \frac{I_A}{\gamma}}{I_{D_{monomer}}}\right) \quad (8)$$

As mentioned above, γ is an instrument specific correction factor which accounts for different quantum yields and detection efficiencies of the donor and acceptor (0.65 here). To extract the binding curves of Hsp70 to tau aggregates of different apparent oligomer sizes, donor events were binned into the indicated size ranges and their association was calculated as described above. For the fibrillar sample, a minimum threshold of 10 monomers per aggregates was applied.

TIRF microscope and data analysis

TIRF microscope. The samples were imaged using a home-built total internal reflection fluorescence microscope. The total internal reflection mode restricts the fluorescence illumination to within 200 nm from the sample slide. A 405 nm laser (Oxxius LaserBoxx), a 488 nm laser (Cobolt MLD) and a 647 nm laser (Cobolt MLD) were aligned and directed parallel to the optical axis at the edge of a 1.49 numerical aperture TIRF objective (APON60XO TIRF, Olympus), mounted on an inverted Nikon Eclipse Ti microscope. Fluorescence was collected by the same objective and separated from the returning TIRF beam by an appropriate dichroic (Di01-R405/488/532/635, Semrock), and passed through appropriate emission filters (AF405: FF01-434/17-25; AF488 and pFTAA: FF03-525/50-25; AF647: LP02-647RU-25. All purchased from Semrock). The control of the hardware was performed using custom-written scripts (bean-shell) for MicroManager (NIH). The images were recorded on an EMCCD camera (Evolve 512 Delta, Photometrics) operating in frame transfer mode (EMGain of 4.4 e–/ADU and 250 ADU/photon). Each pixel was 240 nm in length. Images were recorded for 30 frames with an exposure time of 50 ms and averaged using ImageJ (NIH) software[9] unless stated otherwise.

Binding stoichiometry analysis. Data analysis was performed using ImageJ[9]; the stacks were first averaged over the 100 frames for each channel and the "Find Maxima" command (based on a plugin contributed by Michael Schmid) was used to detect spots present in the AF405, AF488, and AF647 channels. A standard noise tolerance level was set to differentiate the spots from the background (a change in signal of 100 fluorescent counts was used as a threshold).

The pixel co-ordinates and intensities for the spots identified in the three channels were imported into Igor Pro (Wavemetrics) for further analysis. Oligomers were first differentiated from monomeric protein by selecting only those puncta in the AF647 channel that also had a corresponding spot in the AF488 channel (within three pixels of each other). The size of the oligomers was approximated according to equation 9:

$$\text{approximate size} = \frac{I_{G,\text{oligomer}}}{I_{G,\text{monomer}}} + \frac{I_{R,\text{oligomer}}}{I_{R,\text{monomer}}} \quad (9)$$

where $I_{G,\text{oligomer}}$ and $I_{r,\text{oligomer}}$ are the intensities of the coincident spot in the AF488 and AF647 channel, respectively, and $I_{G,\text{monomer}}$ and $I_{r,\text{monomer}}$ are the mean intensities of the non-coincident spots in the AF488 and AF647 channels, respectively. Similar analysis was then performed between the oligomeric puncta and the AF405 spots to determine which oligomers were bound by Hsp70. The approximate number of Hsp70 molecules present per oligomer was calculated using the following equation:

$$\text{approximate number of HSP70 molecules} = \frac{I_{B,\text{coinc}}}{I_{B,\text{noncoinc}}} \quad (10)$$

Where $I_{B,\text{coinc}}$ corresponds to the intensity of each coincident spot, and $I_{B,\text{noncoinc}}$ is the mean intensity from the non-coincident spots. The stoichiometries were then calculated by dividing the approximate number of Hsp70 molecules by the approximate size of the oligomer.

References

1. Meisl, G. *et al*. Molecular mechanisms of protein aggregation from global fitting of kinetic models. *Nat. Protoc*. **11,** 252–272 (2016).
2. Flagmeier, P. *et al*. Mutations associated with familial Parkinson's disease alter the initiation and amplification steps of α-synuclein aggregation. *Proc. Natl. Acad. Sci. U. S. A.* **113,** 10328–10333 (2016).
3. Horrocks, M. H. *et al*. Single Molecule Fluorescence under Conditions of Fast Flow. *Anal. Chem*. **84,** 179–185 (2012).
4. Orte, A., Clarke, R., Balasubramanian, S. & Klenerman, D. Determination of the fraction and stoichiometry of femtomolar levels of biomolecular complexes in an excess of monomer using single-molecule, two-color coincidence detection. *Anal. Chem*. **78,** 7707–7715 (2006).
5. Narayan, P. *et al*. Single molecule characterization of the interactions between amyloid-β peptides and the membranes of hippocampal cells. *J. Am. Chem. Soc*. **135,** 1491–1498 (2013).
6. Narayan, P. *et al*. The extracellular chaperone clusterin sequesters oligomeric forms of the amyloid-β(1-40) peptide. *Nat. Struct. Mol. Biol*. **19,** 79–83 (2012).
7. Cremades, N. *et al*. Direct Observation of the Interconversion of Normal and Toxic Forms of α-Synuclein. *Cell* **149,** 1048–1059 (2012).
8. Swillens, S. Interpretation of binding curves obtained with high receptor concentrations: practical aid for computer analysis. *Mol. Pharmacol*. **47,** 1197–1203 (1995).
9. Schneider, C. A., Rasband, W. S. & Eliceiri, K. W. NIH Image to ImageJ: 25 years of image analysis. *Nat. Methods* **9,** 671–675 (2012).